Mount Abbot Quadrangle, Central Sierra Nevada, California— Analytic Data

GEOLOGICAL SURVEY PROFESSIONAL PAPER 774–C

Mount Abbot Quadrangle, Central Sierra Nevada, California— Analytic Data

By JOHN P. LOCKWOOD

SHORTER CONTRIBUTIONS TO GENERAL GEOLOGY

GEOLOGICAL SURVEY PROFESSIONAL PAPER 774–C

UNITED STATES GOVERNMENT PRINTING OFFICE, WASHINGTON : 1975

UNITED STATES DEPARTMENT OF THE INTERIOR

GEOLOGICAL SURVEY

V. E. McKelvey, *Director*

Library of Congress Cataloging in Publication Data

Lockwood, John P.
Mount Abbot quadrangle, central Sierra Nevada, California–Analytic data. (Shorter contributions to general geology)

(Geological Survey Professional Paper 774–C)
Bibliography: p. C18.
Supt. of Docs. No. I 19.16:774–C
1. Geology–California–Mount Abbot region. I. Title. II. Series: United States. Geological Survey. Shorter contributions to general geology. III. Series: United States. Geological Survey Professional Paper 774–C.
QE90.M77L6 557.94'82 75–61913

For sale by the Superintendent of Documents, U.S. Government Printing Office
Washington, D.C. 20402

Stock Number 024-001-02736-4

CONTENTS

ILLUSTRATIONS

TABLES

MOUNT ABBOT QUADRANGLE, CENTRAL SIERRA NEVADA, CALIFORNIA—ANALYTIC DATA

By JOHN P. LOCKWOOD

ABSTRACT

Modal compositions and specific gravities were determined for 329 samples of granitic rocks of the Mount Abbot quadrangle, California, and 23 selected granitic, volcanic, and metamorphic rocks were chemically and spectrographically analyzed. Modal data and specific gravities plotted on simplified geologic maps supplement the published geologic map of the quadrangle. Most of these data, except for specific gravities, do not show systematic, contourable variation within plutons.

The largest pluton within the quadrangle, occupying an area of about 100 mi² (260 km²), is the highly porphyritic quartz monzonite of Mono Recesses. Alkali feldspar megacrysts are concentrated near the borders of the pluton. Megacrysts also increase in abundance with increasing elevation, which may indicate that the roof of this pluton was originally not too far above present erosional levels. Specific gravities and chemical analyses of samples show that the pluton is weakly zoned, with the densest and most basic rocks located along the highly porphyritic borders. A plot of megacryst abundance versus matrix alkali feldspar content shows an irregular but generally inverse relation between the two, indicating that total alkali feldspar abundance was not the controlling factor in the growth of giant (up to 8 cm) megacrysts. The concentration of megacrysts in the more basic, marginal areas of the pluton indicates either that the bulk composition of the granodiorite magma was appropriate for growth of giant alkali feldspar megacrysts in these areas or that processes especially conducive to their growth operated near pluton borders.

INTRODUCTION

The Mount Abbot quadrangle covers about 240 mi² (620 km²) of dominantly alpine terrain lying across the high crest of the Sierra Nevada between Fresno and Bishop, California. The John Muir Trail crosses the quadrangle from north to south, and the area is visited and traversed by thousands of visitors each summer. The quadrangle lies near the center of an area of the central Sierra Nevada that has been intensively studied geologically over the past three decades (Bateman and others, 1963; Bateman and Eaton, 1967).

This paper was prepared for use with the Geologic Map of the Mount Abbot quadrangle (Lockwood and Lydon, 1975). It summarizes results of laboratory investigations conducted on samples collected in conjunction with geologic mapping of the quadrangle and is part of a continuing study of the bedrock geology of the Sierra Nevada batholith.

GENERAL GEOLOGY

The geologic history of the quadrangle is briefly summarized in a text that accompanies the Geologic Map of the Mount Abbot quadrangle (Lockwood and Lydon, 1975). A generalized small-scale version of this map is given in figure 1. The oldest rocks of the quadrangle are Paleozoic marine sedimentary rocks principally along the north boundary of the quadrangle. Mesozoic volcanic rocks lie along the north boundary and in the southeast quarter of the quadrangle, where they are highly deformed and metamorphosed. These older metamorphic rocks are intruded by Mesozoic granitic rocks that range in composition from diorite to alaskite. Granitic rocks constitute about 95 percent of the bedrock in the quadrangle. The granitic and metamorphic rocks are overlain by volcanic flows of late Tertiary age and by unconsolidated glacial and alluvial deposits of Quaternary age.

ANALYTIC DATA

During the course of geologic mapping, about 400 bedrock samples were collected, 329 of them granitic. The specific gravity and modal mineral composition of these 329 samples were determined. For modal analysis, the samples were sawed into slabs with flat surfaces of at least 40 cm²; these slabs were then stained so that the two feldspars could readily be distinguished from each other and from quartz. The mineral constituents (quartz, alkali feldspar, plagioclase, and mafic minerals) present at each of 1,000–2,000 regularly spaced points on each slab were then observed with a microscope and tabulated. The volume percentages of these minerals were then calculated for each sample locality; the values are shown on simplified bedrock geologic maps of the quadrangle (figs. 2–5) and are given in table 1.[1] The locations of all points for which modes are available are given in figure 6. Individual modes and specific gravities are given in table 2, along with

[1]Modes and specific gravities of samples from smaller plutons are not plotted in figures 2–5 and 7 in order to conserve space; they are given in table 2.

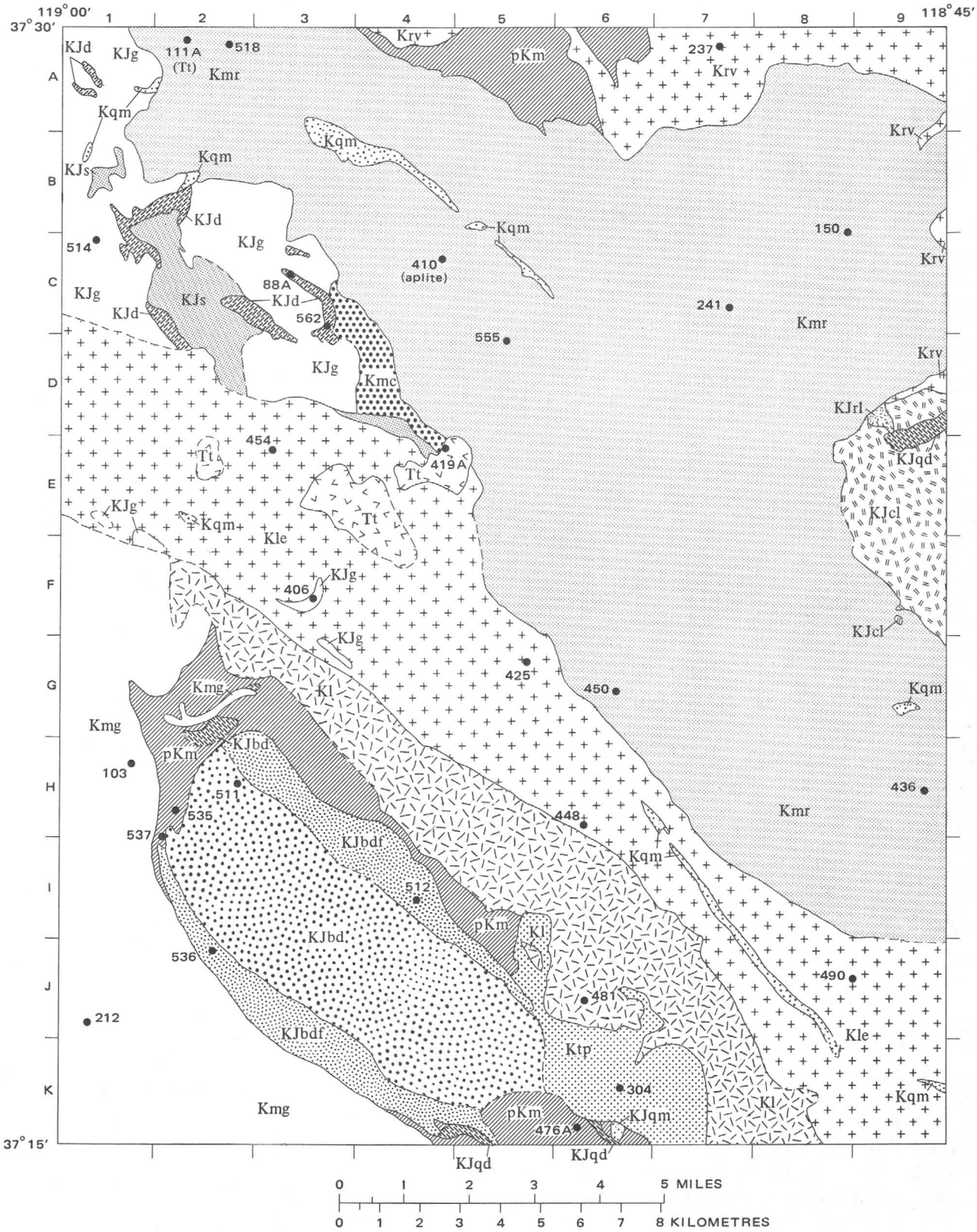

FIGURE 1.—Generalized bedrock geologic map of the Mount Abbot quadrangle showing locations of chemically analyzed samples.

EXPLANATION

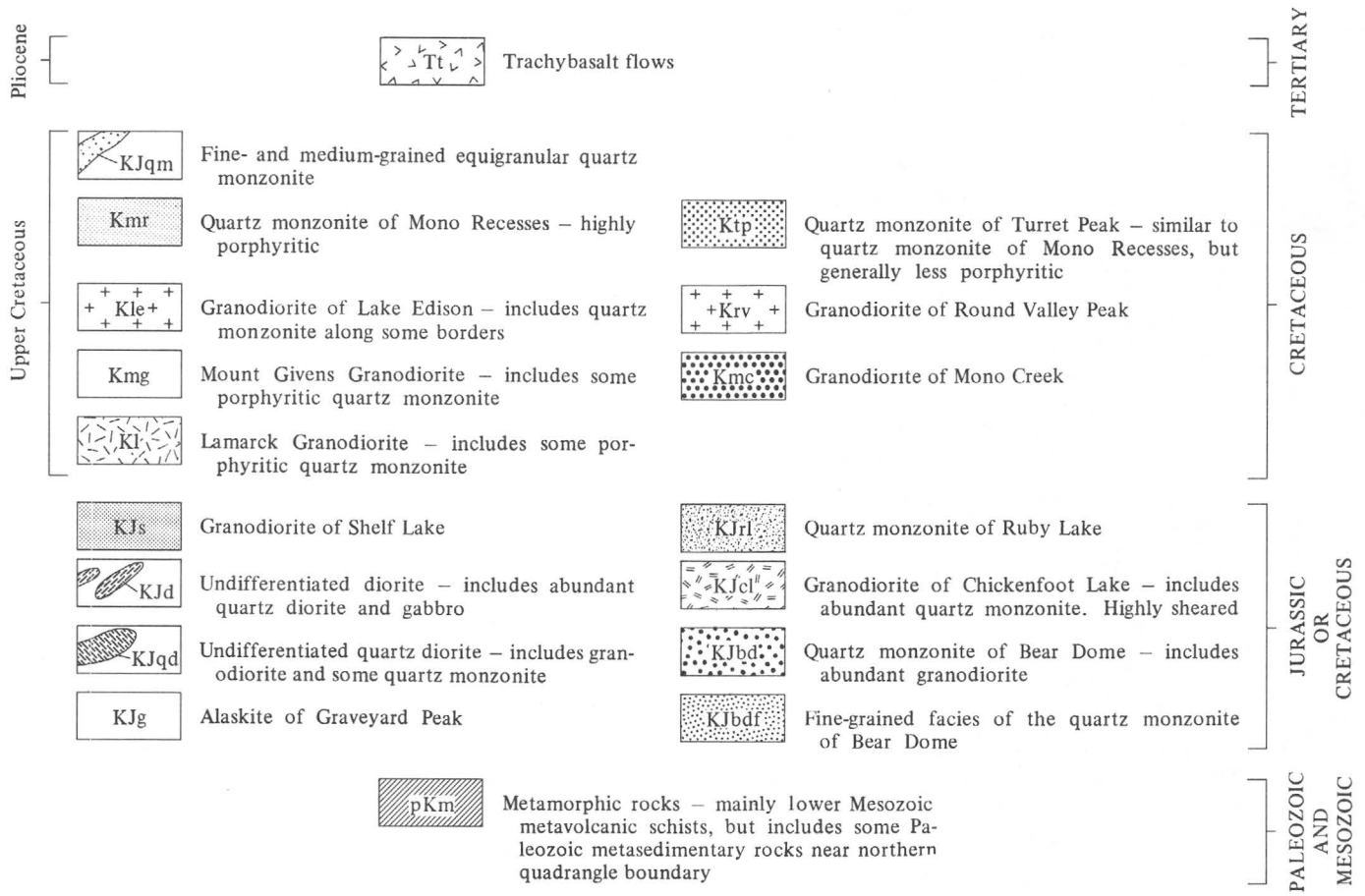

grid coordinates for all sample localities shown on figure 6. Specific gravities and a contour map of the specific gravity data are given in figure 7. The modal data (figs. 2–5) were considered too variable for meaningful contours to be drawn and therefore were not contoured.

In addition to the modal analyses of granitic rocks, 23 samples of granitic rocks from 9 different plutons and 3 dikes, 3 samples of pregranitic metavolcanic rocks, and 2 samples of Tertiary volcanic rocks were analyzed chemically by the rapid method of Shapiro and Brannock (1962). The locations of the chemically analyzed samples are shown in figure 1. These data, together with semiquantitative spectrographic analyses, CIPW norms, and modes of the chemically analyzed granitic rocks are given in table 1.

The modes of the granitic rocks, normalized to 100 percent, are plotted on ternary diagrams (fig. 8), whose corners are quartz, plagioclase, and alkali feldspar. Norms of the chemically analyzed samples are plotted on a ternary diagram whose corners are normative quartz, plagioclase (albite plus anorthite), and orthoclase. All ternary plots were computer-generated. Additional analytic data (mostly spectrographic analyses) are given for stream sediments and some bedrock in the western half of the Mount Abbot quadrangle by Lockwood, Bateman, and Sullivan (1972).

MINERALOGICAL AND COMPOSITIONAL VARIATION IN THE QUARTZ MONZONITE OF MONO RECESSES

The quartz monzonite of Mono Recesses is a large pluton of coarsely porphyritic quartz monzonite and granodiorite that underlies most of the northeastern half of the Mount Abbot quadrangle (Lockwood and Lydon, 1975). This pluton resembles the well-known Cathedral Peak Granite, a granitic pluton located 60 km to the northwest (Bateman and others, 1963, pl. 1), although it is typically not as coarse grained. The distribution of alkali feldspar megacrysts[2] in the quartz monzonite of Mono Recesses was studied in detail. Because the megacrysts are typically large (averaging about 25 × 14 mm in cross-section dimensions) and are

[2]The large alkali feldspar crystals are deliberately termed megacrysts in this report to avoid any connotation of the time of their genesis in their name. The megacrysts have, however, been involved in movement of their host magma, are unquestionably of late-stage magmatic origin, and could doubtless be termed phenocrysts.

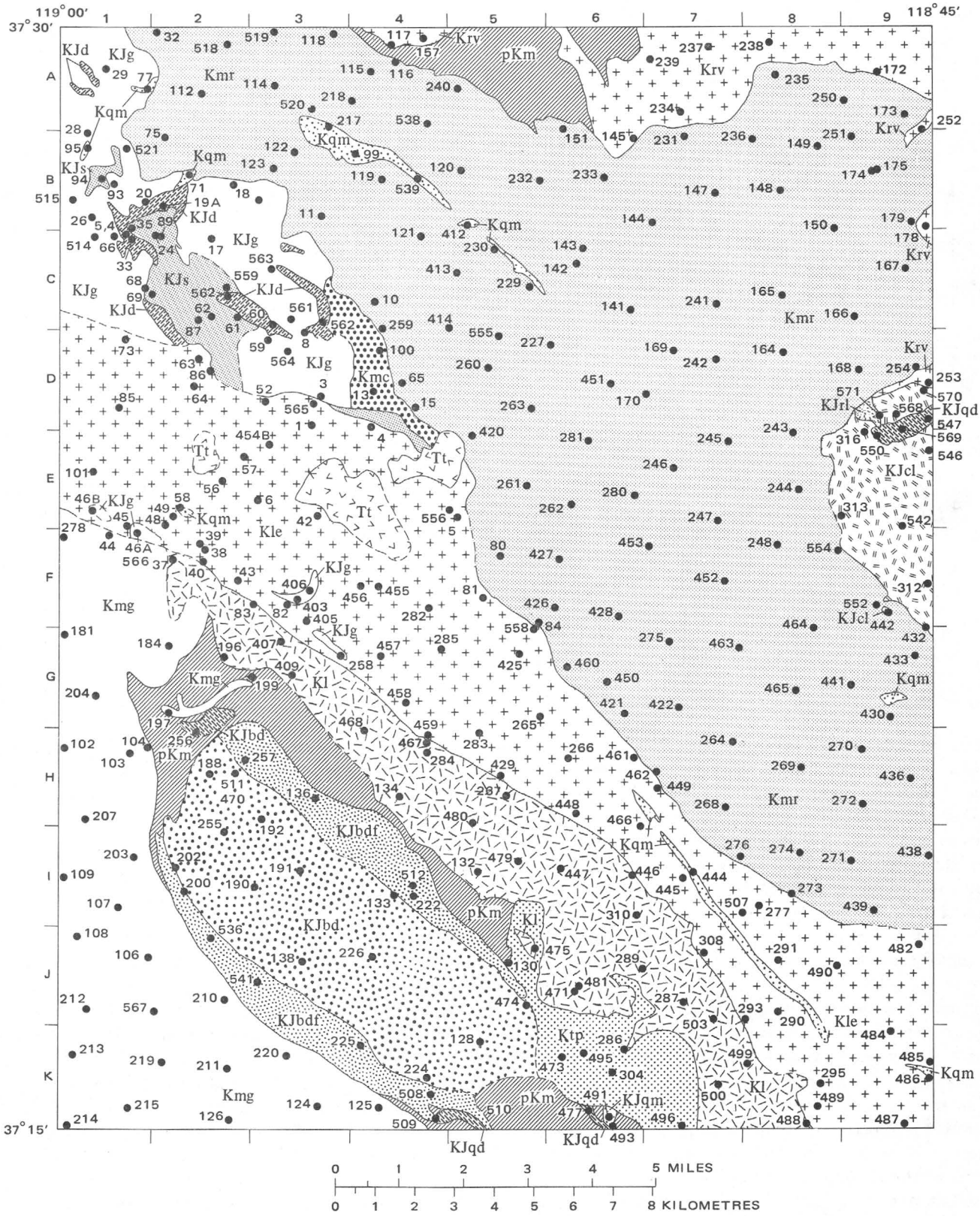

FIGURE 2.—Generalized bedrock geologic map of the Mount Abbot quadrangle showing locations of modally analyzed granitic rock samples.

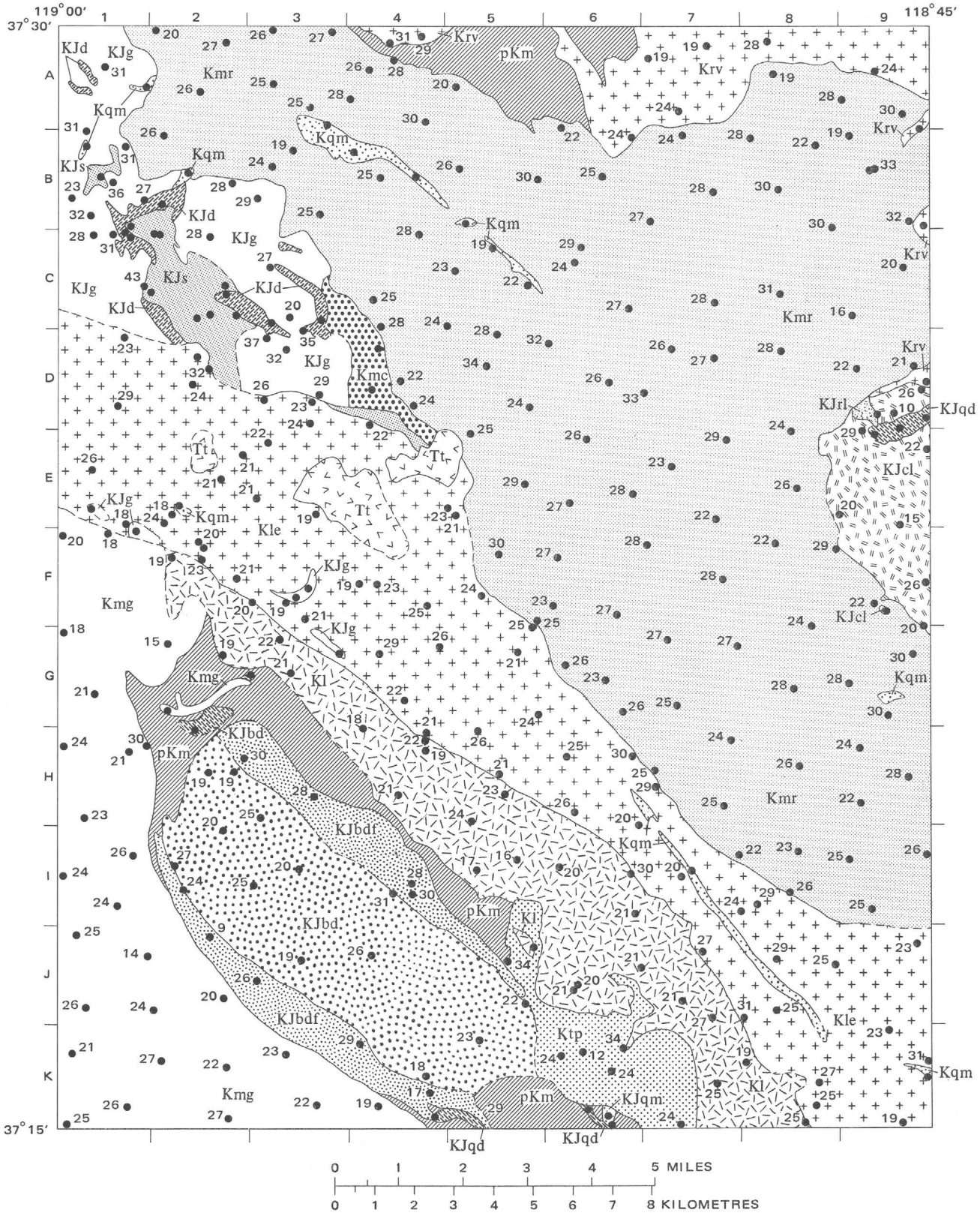

FIGURE 3.—Generalized bedrock geologic map of the Mount Abbot quadrangle showing quartz in granitic rocks in volume percent.

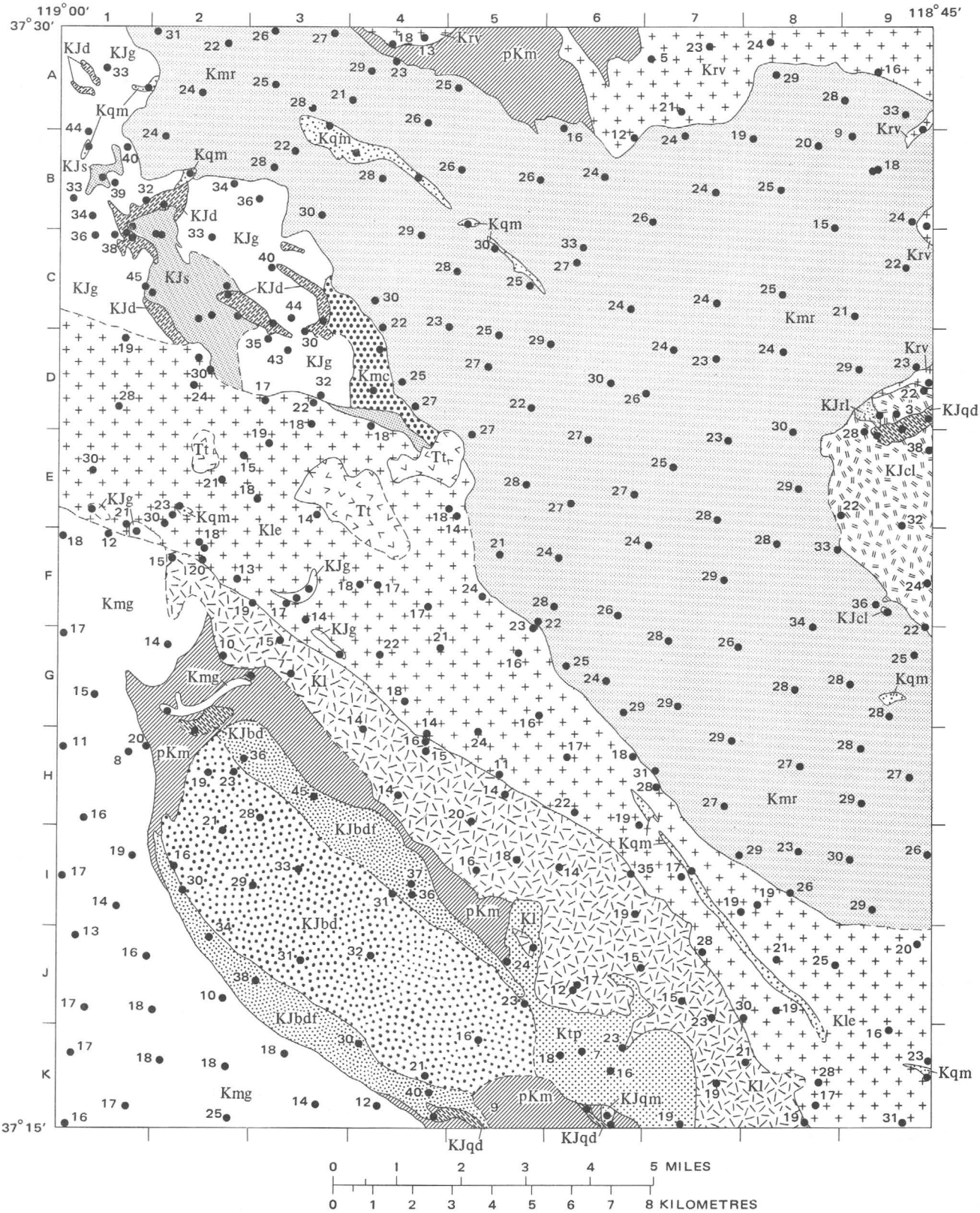

FIGURE 4.—Generalized bedrock geologic map of the Mount Abbot quadrangle showing alkali feldspar in granitic rocks in volume percent.

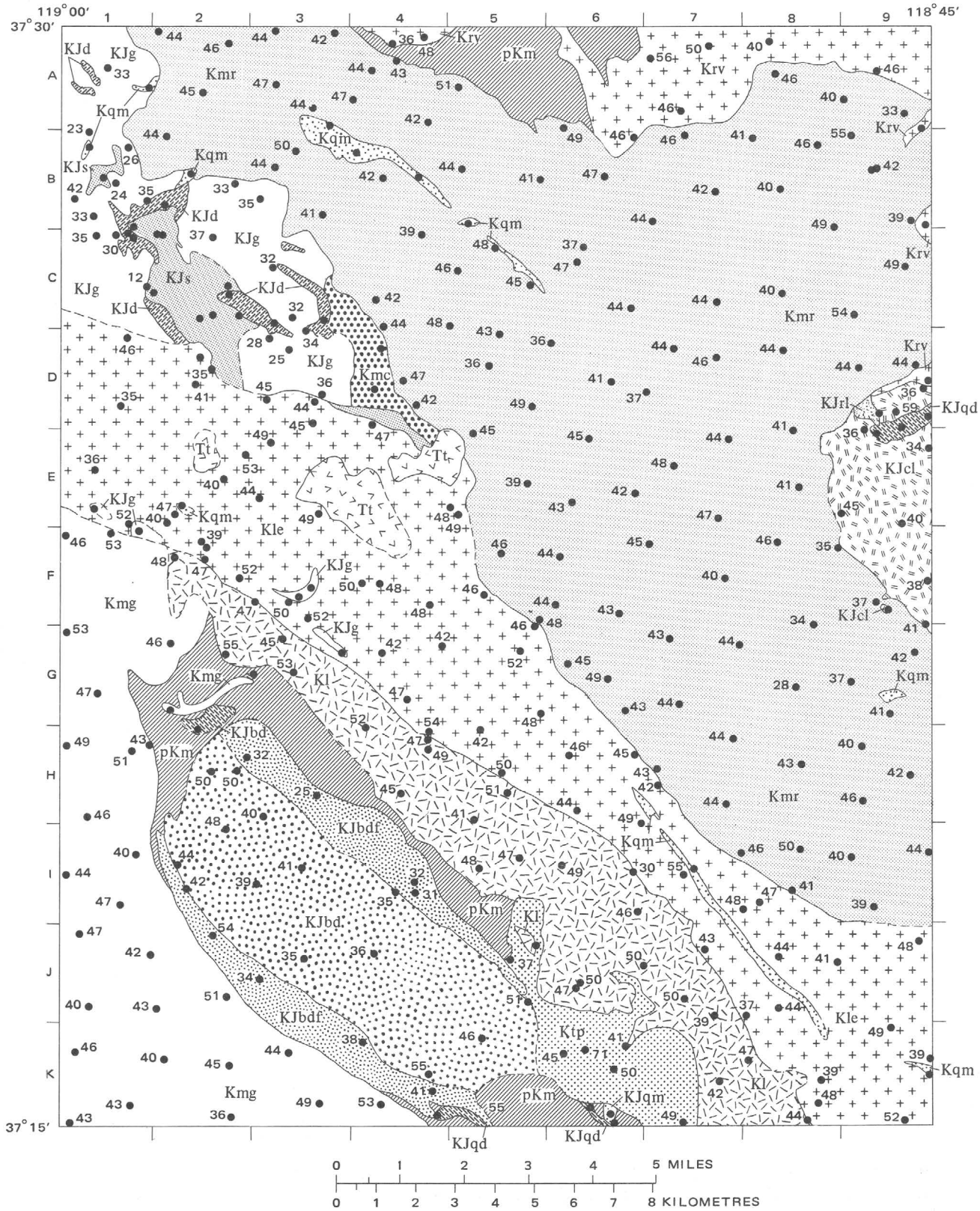

FIGURE 5.—Generalized bedrock geologic map of the Mount Abbot quadrangle showing plagioclase in granitic rocks in volume percent.

TABLE 1.—*Chemical analyses, norms, and modes of rocks*

	Mount Givens Granodiorite		Quartz monzonite of Mono Recesses						Granodiorite of Round Valley Peak	Quartz monzonite of Turret Peak	Granodiorite of Lake Edison			
	A–103	A–212	A–150	A–241	A–436	A–450	A–518	A–555	A–237	A–304	A–425	A–448	A–454B	A–490
Chemical analyses (weight percent)[1]														
SiO_2	61.7	66.0	67.1	71.3	72.1	70.2	70.0	70.6	68.4	64.5	66.1	66.7	66.4	68.8
Al_2O_3	16.9	16.0	15.8	15.0	14.7	15.2	15.2	15.1	15.2	15.8	16.0	16.1	15.7	15.4
Fe_2O_3	2.3	1.6	2.0	1.1	1.1	.00	1.4	1.5	1.6	1.9	2.1	1.6	1.0	1.7
FeO	3.4	2.6	1.4	.96	.76	2.2	.96	1.0	1.8	2.6	2.0	2.2	2.8	1.4
MgO	2.4	1.8	1.0	.50	.31	.70	.50	.65	1.4	1.8	1.4	1.5	1.8	1.1
CaO	5.3	3.7	3.3	2.1	1.7	2.6	2.1	2.4	3.4	3.9	3.9	3.5	3.7	2.9
Na_2O	3.3	3.1	4.0	3.9	3.8	4.0	3.8	3.9	3.3	3.5	3.8	3.5	3.5	3.4
K_2O	2.5	3.4	3.2	4.1	4.3	3.5	3.8	3.8	3.6	3.2	3.3	3.7	3.3	3.9
H_2O+	.91	.74	1.1	.46	.37	.67	1.2	.37	.68	1.0	.53	.31	.80	.70
H_2O-	.19	.18	.23	.08	.08	.00	.05	.11	.09	.30	.12	.07	.05	.09
TiO_2	.73	.57	.47	.27	.23	.36	.32	.39	.40	.55	.55	.44	.49	.39
P_2O_5	.19	.15	.20	.13	.11	.13	.12	.05	.15	.19	.20	.16	.15	.17
MnO	.09	.10	.06	.02	.10	.05	.06	.04	.10	.08	.07	.08	.08	.10
CO_2	<.05	<.05	<.05	<.05	<.05	<.05	<.05	<.05	<.05	<.05	<.05	<.05	<.05	<.05
Sum	100	100	100	100	100	100	100	100	100	100	100	100	100	100
Semiquantitative spectrographic analyses[2]														
B	----	----	----	----	----	----	----	----	----	----	----	----	----	----
Ba	1000	1000	1000	1500	1500	1500	1500	1000	1500	1000	1500	1500	1500	1500
Be	----	----	----	----	3	----	1.5	----	----	----	----	----	----	----
Ce	----	100	----	100	----	----	----	100	100	100	100	100	----	----
Co	20	10	7	3	----	3	2	5	7	15	10	10	10	7
Cr	20	10	3	2	1	1.5	1	2	10	10	7	7	10	5
Cu	30	10	15	7	7	3	3	15	20	10	7	10	10	3
Ga	30	20	20	20	30	20	30	20	20	20	20	15	15	20
La	30	50	30	30	----	30	30	50	70	50	50	50	50	----
Nb	7	10	10	7	7	10	7	10	7	7	10	7	10	7
Nd	----	----	----	----	----	----	----	----	----	----	----	----	----	----
Ni	10	5	----	----	----	----	----	----	5	7	3	3	7	2
Pb	30	30	30	30	50	15	30	20	30	20	20	15	10	30
Sc	20	15	5	2	----	2	2	3	7	10	7	7	7	5
Sr	700	500	1000	700	700	700	1000	1000	700	1000	1000	1000	700	700
V	150	100	70	30	15	30	30	50	700	100	70	70	100	50
Y	30	20	10	10	----	7	10	10	15	15	15	10	20	10
Yb	3	3	1	.7	.7	----	----	1	1.5	1.5	1.5	1	1.5	1
Zr	150	100	150	70	100	100	150	150	70	50	150	100	100	70
CIPW norms (weight percent)														
Q	17.3	23.6	23.6	27.9	29.7	25.8	28.5	27.4	25.8	20.5	21.2	22.0	21.6	26.4
c	----	.85	.24	.64	1.0	.42	1.3	.33	.05	----	----	.36	.002	.72
or	14.8	20.1	19.0	24.3	25.5	20.8	22.6	22.5	21.3	19.1	19.5	21.9	19.6	23.1
ab	28.0	26.3	34.0	33.1	32.3	34.0	32.3	33.1	27.9	29.9	32.2	29.7	29.7	28.8
an	24.0	17.4	15.1	9.6	7.7	12.1	9.7	11.6	15.9	18.1	16.9	16.4	17.4	13.3
ne	----	----	----	----	----	----	----	----	----	----	----	----	----	----
wo	.5	----	----	----	----	----	----	----	----	.07	.50	----	----	----
en	6.0	4.5	2.5	1.2	.78	1.8	1.3	1.6	3.5	4.5	3.5	3.7	4.5	2.7
fs	3.3	2.7	.26	.45	.29	3.6	.19	.03	1.5	2.5	1.2	2.1	3.7	.71
fo	----	----	----	----	----	----	----	----	----	----	----	----	----	----
fa	----	----	----	----	----	----	----	----	----	----	----	----	----	----
mt	3.3	2.3	2.9	1.6	1.6	----	2.0	2.2	2.3	2.8	3.0	2.3	1.5	2.5
hm	----	----	----	----	----	----	----	----	----	----	----	----	----	----
il	1.4	1.1	.90	.51	.44	.69	.61	.7	.76	1.1	1.0	.84	.93	.74
ap	.45	.36	.48	.31	.26	.31	.29	.12	.36	.45	.47	.38	.36	.40
cc	----	----	----	----	----	----	----	----	----	----	----	----	----	----
hl	----	----	----	----	----	----	----	----	----	----	----	----	----	----
fr	----	----	----	----	----	----	----	----	----	----	----	----	----	----
Modes (volume percent)[3]														
Quartz	21.2	26.4	29.7	28.3	30.1	24.2	28.0	30.1	18.6	23.8	21.4	25.6	21.5	25.3
K-feldspar	8.4	17.2	*17.5	*23.5	*22.9	*21.3	*20.3	*18.8	22.6	15.8	15.7	22.2	19.4	25.3
Plagioclase	50.8	40.0	47.7	43.9	44.5	50.8	47.7	46.8	50.4	49.6	52.0	44.3	48.8	41.2
Mafic minerals	19.6	16.4	5.1	4.3	2.5	3.7	4.0	4.3	8.4	10.8	10.9	7.9	10.3	8.2

[1]Rapid-rock analyses (Shapiro and Brannock, 1962) by L. Artis, S. Botts, G. Chloe, P. Elmore, J. Glenn, J. Kelsey, and H. Smith under the supervision of L. Shapiro.

[2]All analyses performed in the laboratory and under the supervision of Harry Bastron. All values in ppm. Looked for but not found: Ag, As, Au, Bi, Cd, Ge, Hf, Hg, In, Li, Mo, Pd, Pt, Re, Sb, Ta, Te, Th, Ti, U, W, Zn. Results reported in percent to the nearest number in the series 1, 0.7, 0.5, 0.3, 0.2, 0.15, and 0.1, etc., which represents approximate midpoints of group data on a geometric scale. The assigned group for semiquantitative results will include the quantitative value for about 30 percent of the analyses.

[3]Analyst: O. K. Polovtzoff.

*Includes alkali feldspar present as phenocrysts in stained slab. For percentages of alkali feldspar present in matrix and as phenocrysts, see table 2.

irregularly distributed at hand specimen scale, their relative abundance is difficult to measure, and so a special field counting method was devised to obtain approximate percentages of megacrysts quickly at selected outcrops in conjunction with geologic mapping.

In this method, appropriately exposed and weathered outcrops were found in which megacrysts could be plainly seen, the number of megacrysts per given area (a map folder 30 by 27 cm in size) were counted, and then the average length of megacrysts in the counted area

TABLE 1.—*Chemical analyses, norms, and modes of rocks*—Continued

	Quartz monzonite of Bear Dome	Quartz monzonite of Jackass Pike		Alaskite of Graveyard Peak		Lamarck Granodiorite	Aplite dike	Diorite dike		Mafic metavolcanic schist		Felsic metavolcanic schist	Trachybasalt	
	A–511	A–512	A–536	A–514	A–406	A–481	A–410	A–88A	A–562	A–535	A–476A	A–537	A–111A	A–419A
Chemical analyses (weight percent)														
SiO_2	68.8	74.9	72.4	76.9	76.1	62.6	76.6	47.7	56.6	70.2	54.0	75.7	50.3	50.3
Al_2O_3	15.3	13.6	14.1	13.0	13.5	16.5	13.1	18.9	17.9	14.9	17.4	12.9	14.9	13.6
Fe_2O_3	1.1	.77	.84	.23	.08	1.5	.40	3.7	2.6	1.1	3.9	.00	2.6	2.7
FeO	1.9	.48	.96	.44	.40	3.7	.20	6.8	4.7	1.7	5.4	.48	5.1	7.0
MgO	.95	.22	.38	.04	.04	2.4	.02	5.1	3.5	1.0	3.9	.03	10.4	9.6
CaO	2.4	.75	1.2	.54	.60	5.0	.70	8.5	6.2	.85	4.4	.07	8.5	8.8
Na_2O	4.0	4.2	4.1	3.3	3.5	3.4	3.5	3.7	3.5	4.0	3.3	1.0	2.7	2.5
K_2O	3.9	4.5	4.3	4.7	4.8	2.9	4.7	1.6	2.0	5.1	3.3	9.0	1.8	2.2
H_2O+	.65	.14	.57	.67	.28	.87	.58	1.3	1.2	.59	1.3	.44	1.5	.85
H_2O-	.06	.05	.05	.07	.05	.03	.03	.13	.17	.05	.10	.05	.58	.35
TiO_2	.44	.19	.28	.06	.07	.64	.05	1.4	.90	.35	1.3	.11	.94	1.2
P_2O_5	.14	.04	.08	.02	.00	.20	.00	.38	.31	.14	.37	.05	.48	.56
MnO	.10	.05	.06	.04	.03	.09	.02	.16	.10	.08	.59	.00	.14	.15
CO_2	<.05	<.05	<.05	<.05	<.05	<.05	<.05	<.05	<.05	<.05	.21	<.05	<.05	<.05
Sum	100	100	99	100	99	100	100	99	100	100	99	100	100	100
Semiquantitative spectrographic analyses														
B	----	----	----	----	10	----	----	----	----	----	----	----	----	----
Ba	1500	1000	2000	200	200	1500	70	500	700	1500	1000	1500	1500	1500
Be	----	1.5	1.5	1.5	3	----	2	----	----	----	1.5	----	----	----
Ce	----	100	100	----	----	----	----	----	----	100	----	----	----	----
Co	7	----	----	----	----	15	----	30	20	7	20	----	50	50
Cr	1.5	----	----	----	----	15	----	10	30	5	50	----	700	700
Cu	2	3	20	3	15	30	10	70	30	.7	1500	10	70	70
Ga	20	20	15	15	15	15	20	20	20	20	20	20	15	15
La	30	50	30	----	----	30	----	----	30	50	----	50	50	50
Nb	7	10	7	50	15	7	----	7	7	7	----	10	7	7
Nd	----	----	----	----	----	----	----	----	----	----	----	----	----	----
Ni	----	----	----	----	----	15	----	30	15	----	15	----	500	300
Ph	10	15	20	30	30	10	50	7	10	15	70	20	19	7
Sc	7	3	3	2	----	15	----	30	15	7	30	----	20	30
Sr	500	150	300	30	30	100	70	1000	1000	300	500	70	1500	1500
V	50	10	10	----	----	150	----	200	100	50	200	----	200	300
Y	20	20	15	50	20	15	----	30	20	15	30	----	20	20
Yb	2	1.5	2	5	3	2	----	3	2	2	3	.7	1.5	2
Zr	100	150	200	70	50	100	20	100	150	200	150	100	100	150
CIPW norms (weight percent)														
Q	23.6	31.5	29.1	38.3	36.0	16.4	36.8	----	9.0	23.7	6.0	35.1	----	----
c	.47	.55	.72	1.6	1.5	----	.98	----	----	1.6	1.8	1.5	----	----
or	23.1	26.6	25.6	27.8	28.5	17.2	27.8	9.5	11.9	30.1	19.6	53.3	10.7	13.1
ab	34.0	35.6	34.9	27.9	29.8	28.8	29.7	28.1	29.8	33.8	28.1	8.5	23.0	21.3
an	11.0	3.5	5.5	2.6	3.0	21.2	3.5	30.5	27.4	3.3	18.2	.021	23.4	19.5
ne	----	----	----	----	----	----	----	1.8	----	----	----	----	----	----
wo	----	----	----	----	----	.96	----	4.0	.63	----	----	----	6.6	8.7
en	2.4	.55	.95	.10	0.10	6.0	.05	2.4	8.8	2.5	9.8	.075	14.8	13.9
fs	2.0	.025	.72	.59	0.61	4.7	----	1.4	5.2	1.8	5.7	.70	3.4	5.2
fo	----	----	----	----	----	----	----	7.3	----	----	----	----	7.9	7.1
fa	----	----	----	----	----	----	----	4.7	----	----	----	----	2.0	2.9
mt	1.6	1.1	1.2	.33	.12	2.2	.57	5.4	3.8	1.6	5.7	----	3.8	3.9
hm	----	----	----	----	----	----	.010	----	----	----	----	----	----	----
il	.84	.36	.54	.11	.13	1.2	.095	2.7	1.7	.66	2.5	.21	1.8	2.3
ap	.33	.095	.19	.047	----	.48	----	.9	.74	.33	.88	.12	1.1	1.3
cc	----	----	----	----	----	----	----	----	----	----	.48	----	----	----
hl	----	----	----	----	----	----	----	----	----	----	----	----	----	----
fr	----	----	----	----	----	----	----	----	----	----	----	----	----	----
Modes (volume percent)														
Quartz	19.3	28.0	8.7	28.0	32.9	20.2	29.0	----	----	----	----	----	----	----
K-feldspar	23.4	37.2	34.3	36.3	35.3	16.6	41.1	----	----	----	----	----	----	----
Plagioclase	49.7	31.8	53.6	35.2	30.3	50.0	29.6	----	----	----	----	----	----	----
Mafic minerals	7.6	3.0	3.4	.5	1.5	13.2	.3	----	----	----	----	----	----	----

was estimated. Then, using 1.73 as an average length-to-width ratio of megacrysts in the quartz monzonite of Mono Recesses (on the basis of measurement of 46 megacrysts), the volume percentage of megacrysts over the area of the map folder is equal to $XY^2/14.01$ where X equals the number of megacrysts per area, and Y equals the average length of the megacryst. This method could be used only on plutons in which the shape of megacrysts is relatively constant; for plutons with megacrysts of variable morphology, both length and width averages must be estimated at each count area.

To check the approximate accuracy of the area-count method, the volume percentages of alkali feldspar megacrysts were determined by point counts at 23 localities where the area counts also were available. Point counts were made by placing a 1,000-point grid of

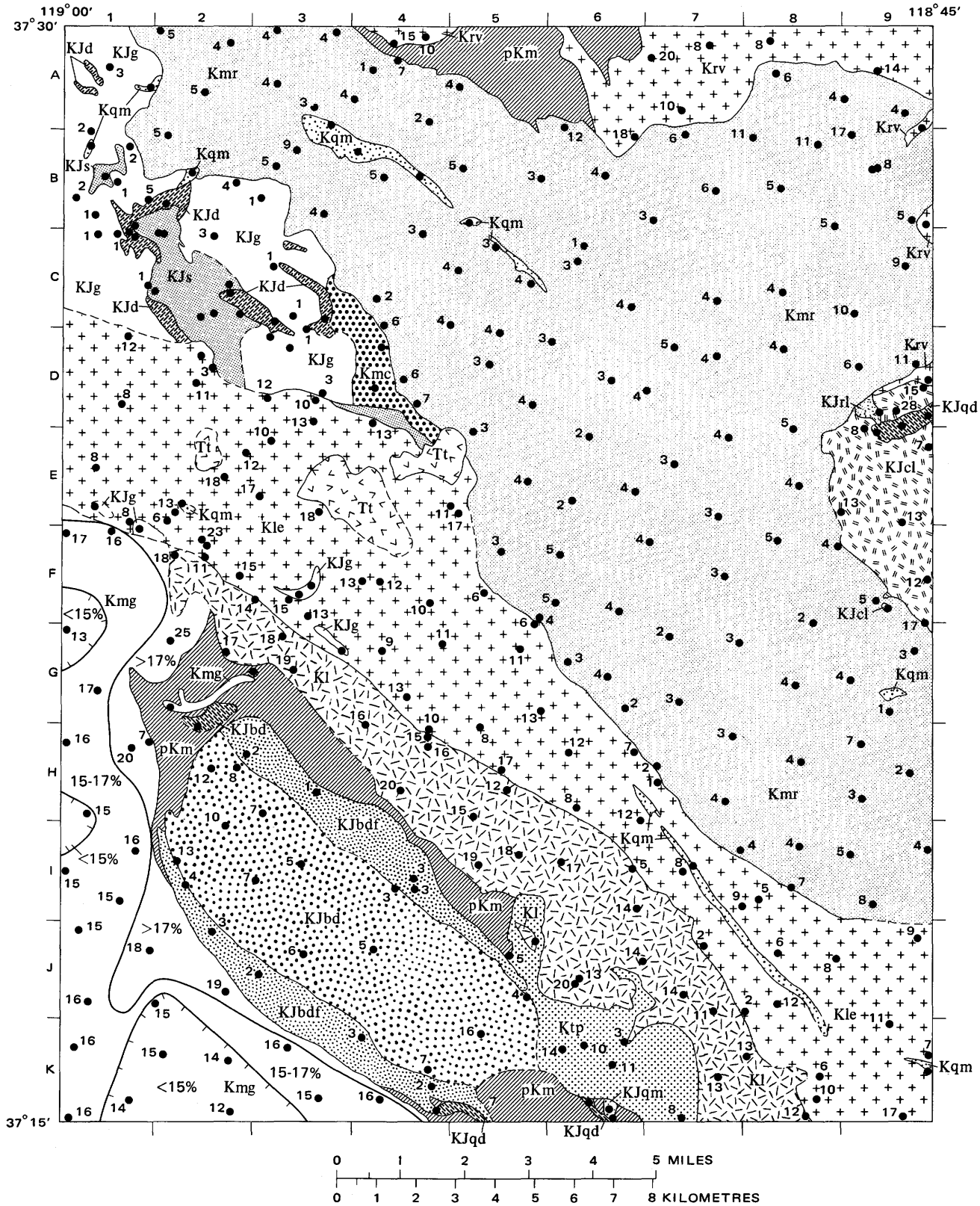

FIGURE 6.—Generalized bedrock geologic map of the Mount Abbot quadrangle showing mafic minerals in granitic rocks in volume percent.

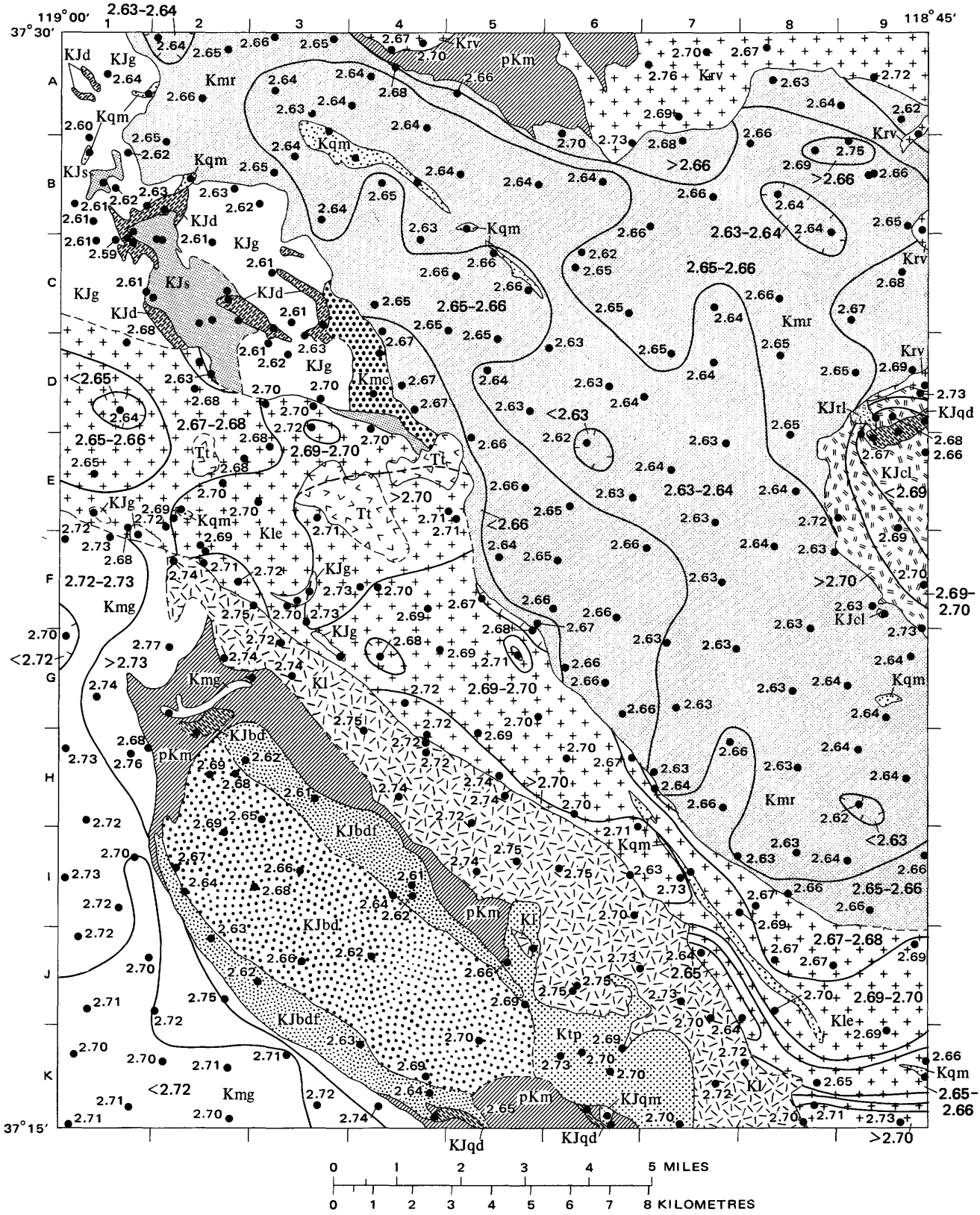

FIGURE 7.—Generalized bedrock geologic map of the Mount Abbot quadrangle showing specific gravity of granitic rocks.

PLOTS OF MODES

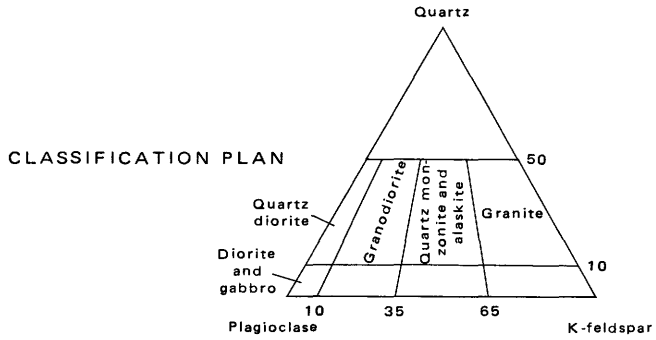

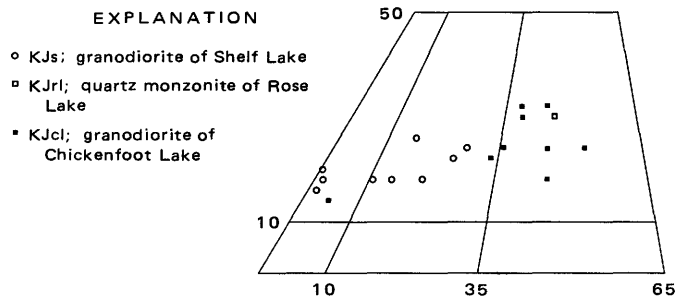

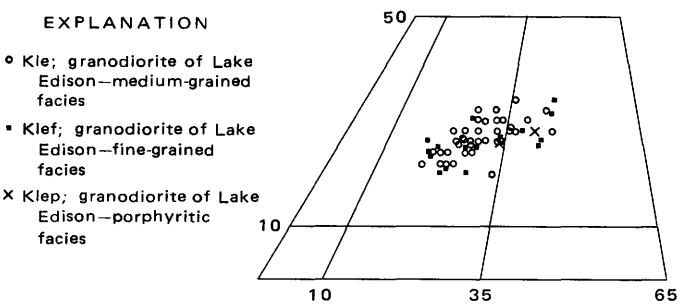

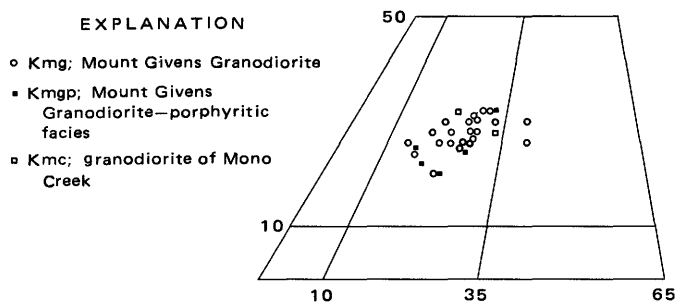

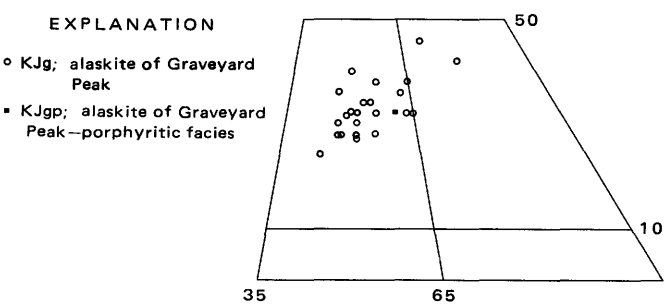

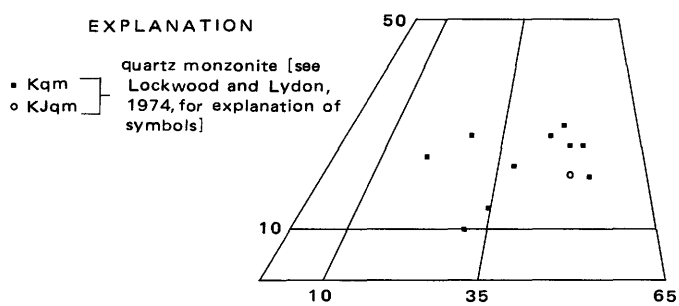

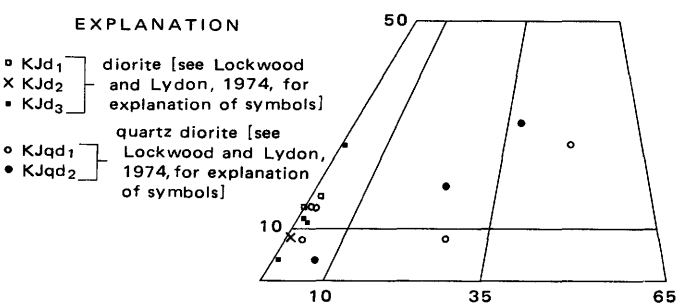

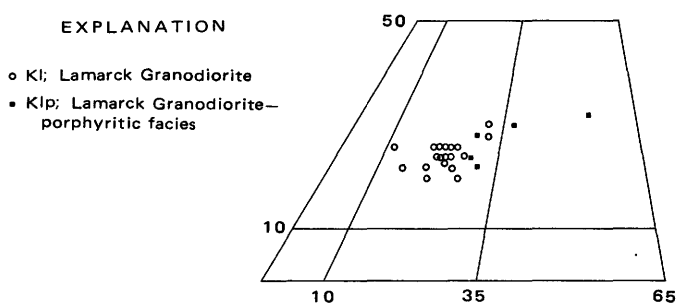

FIGURE 8.—Generalized bedrock geologic map of the Mount

PLOTS OF MODES

EXPLANATION

- ○ Krv; granodiorite of Round Valley Peak

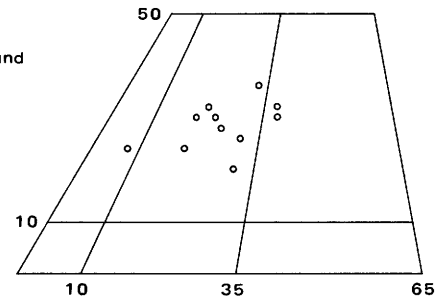

EXPLANATION

- ● Kmr; quartz monzonite of Mono Recesses
- × Ktp; quartz monzonite of Turret Peak

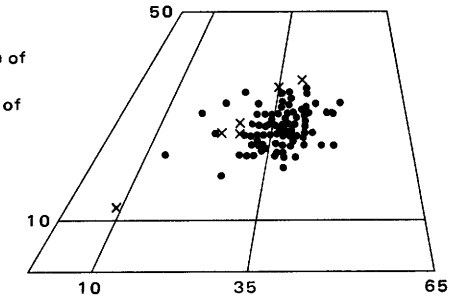

EXPLANATION

- ○ KJbd; quartz monzonite of Bear Dome
- ▪ KJbdf; quartz monzonite of Bear Dome—fine-grained facies

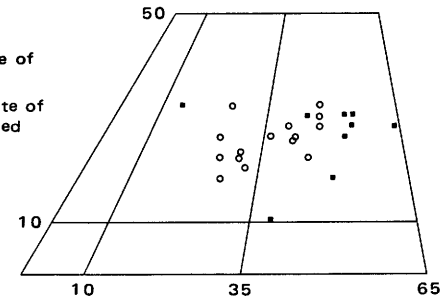

PLOT OF NORMS

EXPLANATION

- ○ Mount Givens Granodiorite
- ● quartz monzonite of Mono Recesses
- ▫ granodiorite of Round Valley Peak
- ▪ quartz monzonite of Turret Peak
- △ granodiorite of Lake Edison
- ▲ quartz monzonite of Bear Dome
- ◇ quartz monzonite of Bear Dome—fine-grained facies
- ◆ alaskite of Graveyard Peak
- ◪ Lamarck Granodiorite
- \+ aplite
- × diorite
- ✱ mafic metavolcanic schist
- # felsic metavolcanic schist
- ✱ trachybasalt

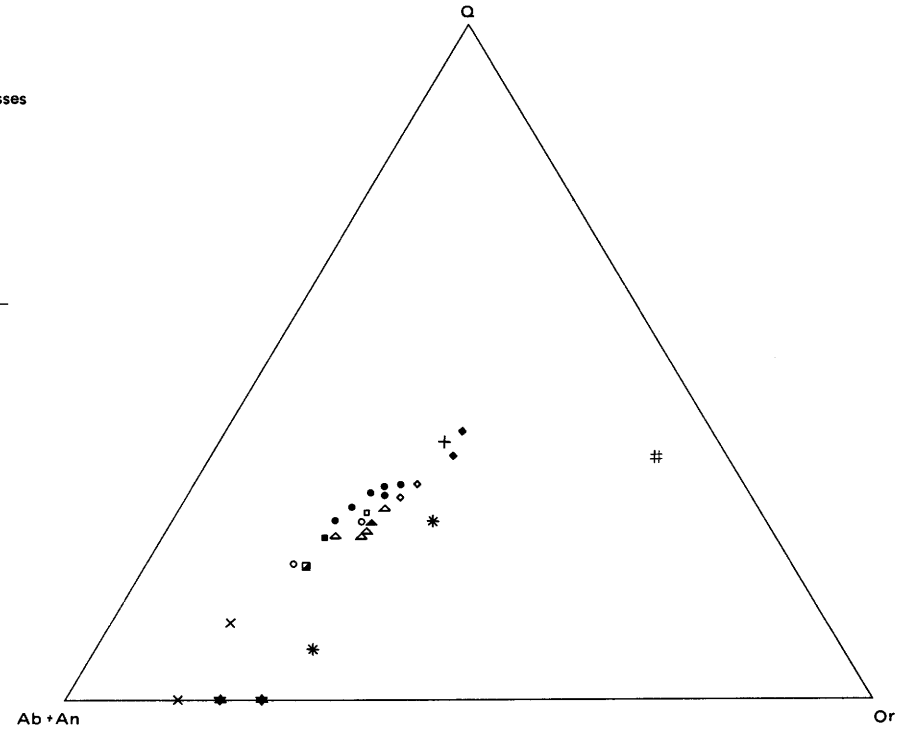

Abbot quadrangle showing ternary plots of modes and norms.

TABLE 2.—*Modes, specific gravities, and grid coordinates of granitic rocks*

Sample No.	Map symbol for rock unit[1]	Coordinates	Modes (percent)					Specific gravity
			Alkali feldspar					
			Plagioclase	Matrix[2]	Megacrysts[3]	Quartz	Mafic minerals	
A–1	Kle	D, 3	44.7	18.1		24.0	13.2	2.715
A–3	KJg	D, 3	36.5	32.2		28.6	2.7	2.695
A–4	Klef	D, 4	47.1	18.3		21.6	13.0	2.699
A–5	Kle	E, 5	48.6	13.5		20.6	17.3	2.710
A–6	Kle	E, 3	44.2	17.6		20.8	17.4	2.700
A–8A	KJg	D, 3	33.9	29.8		35.0	1.3	2.629
A–10	Kmr	C, 4	41.9	19.8	10.7	25.1	2.5	2.649
A–11	Kmr	B, 3	41.2	19.7	10.7	24.7	3.7	2.640
A–13	Kmc	D, 4	42.0	11.6		23.7	12.7	2.680
A–15	Kmr	D, 4	41.6	15.6	12.0	24.0	6.8	2.667
A–17	KJg	C, 2	36.7	32.7		27.7	2.9	2.611
A–18	KJg	B, 2	33.2	34.5		28.4	3.9	2.628
A–19A	KJd3	B, 2	59.6	.5		8.8	31.1	2.830
A–20B	KJg	B, 1	35.3	32.4		27.3	5.0	2.634
A–24	KJs	C, 2	56.1	9.4		14.2	20.3	2.750
A25-4	KJd3	C, 1	65.6	.5		3.2	30.7	2.868
A25-5	KJd2	C, 1	65.5	.7		5.7	28.1	2.865
A–26	KJg	B, 1	32.9	33.6		32.3	1.2	2.610
A–28	KJg	B, 1	23.3	43.8		30.7	2.2	2.600
A–29	KJg	A, 1	33.2	32.7		31.3	2.8	2.642
A–32	Kmr	A, 2	43.6	23.0	7.8	20.4	5.2	2.645
A–33	KJd3	C, 1	64.2	1.1		8.4	26.3	2.820
A–35	KJs	B, 1	45.9	15.5		16.6	22.0	2.755
A–37	Kl	F, 2	47.6	14.6		19.3	18.5	2.745
A–38	Klef	F, 2	39.3	29.9		23.9	6.9	2.644
A–39	Kle	F, 2	39.3	18.1		19.7	22.9	2.690
A–40	Klef	F, 2	46.9	19.6		22.7	10.8	2.711
A–42	Kle	E, 3	49.1	14.1		18.6	18.2	2.710
A–43	Klef	F, 2	51.5	12.6		21.0	14.9	2.720
A–44	Kmgp	F, 1	53.3	12.5		18.2	16.0	2.726
A–45	Klef	E, 1	52.5	21.1		18.1	8.3	2.682
A–46A	KJg	F, 1	16.6	37.6		45.2	.6	2.600
A–46B	KJg	E, 1	29.2	29.0		40.1	1.7	2.630
A–48	Klef	E, 2	40.0	30.0		23.5	6.5	2.668
A–49	Kle	E, 2	46.7	23.1		17.5	12.7	2.690
A–52	Klef	D, 3	45.2	17.4		25.5	11.9	2.705
A–56	Kle	E, 2	40.0	21.0		21.3	17.7	2.701
A–57	Kle	E, 2	52.8	14.8		20.6	11.8	2.682
A–58	Kqm1	E, 2	35.3	33.3		28.9	2.5	2.625
A–59	KJg	D, 3	27.6	35.1		37.0	.3	2.610
A–60	KJd1	C, 3	67.6	.1		10.4	21.9	2.842
A–61	KJs	C, 2	50.0	13.0		14.6	22.4	2.760
A–62	KJs	C, 2	54.5	6.7		12.7	26.1	2.650
A–63A	Klef	D, 2	52.5	15.8		17.4	14.3	2.720
A–64	Kle	D, 2	41.3	23.7		24.4	10.6	2.679
A–65	Kmr	D, 4	47.1	13.9	10.9	22.3	5.8	2.668
A–66	KJg	C, 1	29.7	38.3		31.3	.7	2.594
A–68	KJg	C, 1	11.8	45.0		42.7	.5	2.608
A–69	KJs	C, 1–2	64.9	.0		15.5	19.6	2.770
A–71A	Kqm1	B, 2	33.0	36.4		23.7	6.9	2.643
A–73	Kle	D, 1	45.6	19.4		22.8	12.2	2.682
A–75	Kmr	B, 2	44.5	15.6	8.8	25.7	5.4	2.651
A–77	Kqm1	A, 1	52.4	12.6		21.4	13.6	2.720
A–80	Kmr	F, 5	46.0	10.8	10.3	29.8	3.1	2.641
A–81	Kle	F, 5	45.5	23.9		24.3	6.3	2.671
A–82	Klef	F, 3	50.0	16.6		18.6	14.8	2.704
A–83	Kl	F, 3	47.3	18.9		20.0	13.8	2.750
A–84	Kmr	F, 5	48.4	11.9	10.5	25.3	3.9	2.670
A–85	Kle	D, 1	35.0	28.2		28.6	8.2	2.635
A–86	Klef	D, 2	34.7	29.9		32.4	3.0	2.632
A–87	KJs	C, 2	56.0	1.0		12.5	30.5	2.837
A–89	KJs	C, 2	48.9	10.1		19.6	21.4	2.758
A–90	KJd3	B, 2	55.1	.7		18.9	25.3	2.824
A–93	KJg	B, 1	23.7	38.8		36.2	1.3	2.620
A–94	KJs	B, 1	60.8	.5		12.3	26.4	2.811
A–95	Kqm1	B, 1	36.2	41.8		20.3	1.7	2.622
A–98	KJg	B, 3	34.8	36.0		28.6	.6	2.620
A–99	Kqm1	B, 4	46.1	29.2		21.7	3.0	2.650
A–100	Kmc	D, 4	47.7	14.4		27.9	10.0	2.692
A–101	Kle	E, 1	36.0	30.0		26.3	7.7	2.682
A–102	Kmg	H, 1	48.6	11.4		23.5	16.5	2.729
A–103	Kmg	H, 1	50.8	8.4		21.2	19.6	2.760
A–104	Kmgp	H, 1–2	43.0	20.1		29.5	7.4	2.681
A–106	Kmg	J, 1–2	41.7	16.4		23.9	18.0	2.701
A–107	Kmg	I, 1	46.9	14.2		23.6	15.3	2.721
A–108	Kmg	J, 1	46.6	12.9		25.3	15.2	2.723
A–109	Kmg	I, 1	43.8	16.7		24.4	15.1	2.728
A–112	Kmr	A, 2	44.7	20.1	4.3	26.3	4.6	2.658
A–114	Kmr	A, 3	46.6	18.5	6.3	25.1	3.5	2.643
A–115	Kmr	A, 4	43.5	20.9	8.0	26.3	1.3	2.635
A–116	Kmr	A, 4	42.8	11.7	10.9	27.9	6.7	2.678
A–117	Krv?	A, 4	35.7	17.7		31.2	15.4	2.671
A–118	Kmr	A, 3	41.5	18.7	7.9	27.4	4.5	2.652
A–119	Kmr	B, 4	41.7	23.2	5.0	24.9	5.2	2.650
A–120	Kmr	B, 5	43.6	18.4	7.4	25.7	4.9	2.640
A–121	Kmr	C, 4	39.2	22.6	6.8	28.5	3.1	2.633
A–122	Kmr	B, 3	49.9	15.5	6.6	19.2	8.8	2.637
A–123	Kmr	B, 3	43.5	18.3	9.2	24.2	4.6	2.650
A–124	Kmg	K, 3	49.2	14.1		21.5	15.2	2.724
A–125	Kmg	K, 4	52.9	11.6		19.3	16.2	2.735
A–126	Kmg	K, 2	36.2	24.6		26.7	12.5	2.698
A–128	KJbd	K, 5	45.9	15.8		22.7	15.6	2.698
A–130	Ktp	J, 5	36.8	24.5		34.1	4.6	2.656
A–132	Kl	I, 5	47.5	16.5		17.4	18.6	2.740
A–133	KJbd	I, 4	34.8	30.9		30.9	3.4	2.645
A–134	Kl	H, 4	45.0	13.9		20.8	20.3	2.737
A–136	KJbdf	H, 3	24.9	45.4		28.3	1.4	2.608
A–138	KJbd	J, 3	34.8	30.7		28.9	5.6	2.659
A–141	Kmr	C, 6	44.5	20.2	4.1	27.0	4.2	2.648
A–142	Kmr	C, 6	46.6	23.0	4.0	23.5	2.9	2.649
A–143	Kmr	C, 6	36.6	29.1	4.0	29.0	1.3	2.620
A–144	Kmr	B, 7	44.1	19.7	6.2	26.9	3.1	2.661
A–145	Krv	B, 6	46.5	11.7		23.8	18.0	2.729
A–147	Kmr	B, 7	42.5	12.5	11.2	27.9	5.9	2.657
A–148	Kmr	B, 8	39.9	16.0	9.0	29.7	5.4	2.636
A–149	Kmr	B, 8	46.4	18.8	1.0	22.5	11.3	2.687
A–150	Kmr	B, 8	48.9	7.2	8.2	30.5	5.2	2.641
A–151	Kmr	A, 6	49.4	9.7	6.5	22.0	12.4	2.698
A–157	Krv?	A, 4	47.6	13.0		29.3	10.1	2.699
A–164	Kmr	D, 8	46.3	18.8	5.0	28.2	3.7	2.649
A–165	Kmr	C, 8	39.6	17.2	7.8	31.4	4.0	2.657
A–166	Kmr	C, 9	53.6	10.0	10.8	15.6	10.0	2.674
A–167	Kmr	C, 9	48.7	20.3	2.0	19.8	9.2	2.680
A–168	Kmr	D, 9	43.5	18.2	10.7	22.1	5.5	2.651
A–169	Kmr	D, 7	44.3	20.0	4.4	26.4	4.9	2.653
A–170	Kmr	D, 7	36.8	22.4	4.0	33.3	3.5	2.640
A–172	Krv	A, 9	45.9	16.0		24.1	14.0	2.716
A–173	Kmr	A, 9	33.3	32.7		29.8	4.2	2.625
A–174	Kmr	B, 9	47.2	9.4	1.0	25.6	16.8	2.750
A–175	Kmr	B, 9	41.5	17.0	1.0	32.9	7.6	2.665
A–178A	Krv	B, 9	47.7	11.7		18.9	21.7	2.750
A–179	Kmr	B, 9	39.1	23.0	1.0	31.9	5.0	2.654
A–181	Kmgp	G, 1	52.9	16.8		17.6	12.7	2.704
A–184	Kmg	G, 2	46.5	13.6		15.2	24.7	2.769
A–188	KJbd	H, 2	49.7	19.1		18.8	12.4	2,691
A–190	KJbd	I, 3	39.2	28.9		24.6	7.3	2.679
A–191	KJbd	I, 3	41.3	32.9		20.5	5.3	2.655
A–192	KJbd	H, 3	40.0	27.7		25.3	7.0	2.654
A–196A	Kl	G, 2	55.0	9.8		18.6	16.6	2.737
A–197	Kmg	G, 2	39.2	27.3		22.2	11.3	2.691
A–199	KJqd1	G, 2–3	74.8	2.1		12.6	10.5	2.778
A–200	KJbdf	I, 2	41.9	29.8		23.8	4.5	2.637
A–202	KJbd	I, 2	43.9	16.2		27.3	12.6	2.674
A–203	Kmg	I, 1	39.7	18.8		25.7	15.8	2.702
A–204	Kmg	G, 1	47.4	15.1		20.9	16.6	2.735
A–207	Kmg	H, 1	46.0	16.4		22.7	14.9	2.722
A–210	Kmgp	J, 2	50.7	9.9		20.0	19.4	2.754
A–211	Kmg	K, 2	45.2	18.5		22.1	14.2	2.714
A–212	Kmg	J, 1	40.0	17.2		26.4	16.4	2.710
A–213	Kmg	K, 1	45.8	16.7		21.4	16.1	2.695
A–214	Kmg	K, 1	43.1	16.1		24.8	16.0	2.710
A–215	Kmg	K, 1	43.0	16.6		26.1	14.3	2.709
A–217	Kqm1	A, 3	58.6	26.2		8.8	6.4	2.663
A–218	Kmr	A, 4	47.4	17.2	3.8	27.5	4.1	2.644
A–219	Kmg	K, 2	39.7	18.4		27.1	14.8	2.704
A–220	Kmg	K, 3	43.8	17.6		22.8	15.8	2.714
A–222	KJbdf	I, 4	31.2	36.3		29.7	2.8	2.619
A–224	KJbd	K, 4	54.6	21.3		17.5	6.6	2.688
A–225	KJbdf	K, 4	37.9	29.8		28.9	3.4	2.632
A–226	KJbd	J, 4	36.5	32.3		26.3	4.9	2.625
A–227	Kmr	D, 6	36.3	22.8	6.4	31.5	3.0	2.629
A–229	Kmr	C, 5	48.5	18.8	6.2	22.2	4.3	2.660
A–230	Kmr	C, 5	47.8	25.0	4.8	19.4	3.0	2.661
A–231	Kmr	B, 7	45.8	17.8	6.4	23.8	6.2	2.676
A–232	Kmr	B, 5	40.8	20.2	6.0	29.9	3.1	2.639
A–233	Kmr	B, 6	47.0	16.8	6.7	25.3	4.2	2.635
A–234	Krv	A, 7	46.0	20.7		23.5	9.8	2.689
A–235	Kmr	A, 8	46.0	29.4		19.0	5.6	2.629
A–236	Kmr	B, 8	41.4	15.0	4.2	28.4	11.0	2.665
A–237	Krv	A, 7	50.4	22.6		18.6	8.4	2.697
A–238	Krv	A, 8	40.3	24.5		27.7	7.5	2.674
A–239	Krv	A, 7	56.0	5.1		18.9	20.0	2.760
A–240	Kmr	A, 5	51.0	10.2	14.4	20.4	4.0	2.656
A–241	Kmr	C, 7	43.8	18.4	5.2	28.3	4.3	2.640
A–242	Kmr	D, 7	45.9	19.1	4.1	26.8	4.1	2.638
A–243	Kmr	E, 8	41.1	22.7	7.6	23.6	5.0	2.653
A–244	Kmr	E, 8	41.1	22.8	6.6	26.0	3.5	2.641
A–245	Kmr	E, 7	44.4	16.8	6.2	29.0	3.6	2.634
A–246	Kmr	E, 7	48.5	21.0	4.3	23.0	3.2	2.639
A–247	Kmr	E, 7	47.2	23.3	4.2	22.0	3.3	2.632
A–248	Kmr	F, 8	45.5	23.1	4.5	21.7	5.2	2.644
A–250	Kmr	A, 9	39.5	27.9		28.3	4.3	2.638
A–251	Kmr	B, 9	54.9	9.0		18.9	17.2	2.751
A–252	Krv	A, 9	38.5	23.5		29.5	8.5	2.672
A–253	Krv	D, 9	46.7	15.0		25.2	13.1	2.705
A–254	Kmr	D, 9	44.2	17.6	5.7	21.4	10.9	2.692
A–255	KJbd	I, 2	48.2	21.2		20.4	10.2	2.690
A–256	KJqd1	H, 2	56.2	21.6		7.1	15.1	2.778
A–257	KJbdf	H, 2	32.0	35.7		29.8	2.5	2.617
A–258	KJg	G, 3	30.5	35.0		33.7	.8	2.626
A–259	Kmr	C–D, 4	43.7	11.4	10.9	28.0	6.0	2.668
A–260	Kmr	D, 5	36.4	19.4	7.2	33.6	3.4	2.636
A–261	Kmr	E, 5	38.6	19.5	8.7	29.2	4.0	2.657
A–262	Kmr	E, 6	43.4	19.1	8.2	26.8	2.5	2.648
A–263	Kmr	E, 6	49.1	14.2	8.1	24.3	4.3	2.628

TABLE 2.—*Modes, specific gravities, and grid coordinates of granitic rocks*—Continued

Sample No.	Map symbol for rock unit[1]	Coordinates	Modes (percent)					Specific gravity
			Alkali feldspar					
			Plagioclase	Matrix[2]	Megacrysts[3]	Quartz	Mafic minerals	
A–264	Kmr	H, 7	43.9	25.3	3.9	24.0	2.9	2.656
A–265	Kle	G, 5	47.9	15.5		23.6	13.0	2.705
A–266	Kle	H, 6	46.4	16.8		24.8	12.0	2.698
A–267	Kl	H, 5	50.8	14.4		22.9	11.9	2.736
A–268	Kmr	H, 7	43.9	19.5	7.7	25.0	3.9	2.655
A–269	Kmr	H, 8	43.1	21.9	5.4	26.1	3.5	2.629
A–270	Kmr	H, 9	39.6	24.5	4.0	24.5	7.4	2.636
A–271	Kmr	I, 9	40.2	25.0	5.5	24.6	4.7	2.638
A–272	Kmr	H, 9	45.7	22.6	6.4	22.1	3.2	2.621
A–273	Kmr	I, 8	40.8	14.3	11.9	26.2	6.8	2.659
A–274	Kmr	I, 8	50.1	16.2	7.0	23.1	3.6	2.631
A–275	Kmr	G, 7	43.4	22.8	5.3	26.6	1.9	2.631
A–276	Kmr	I, 7	45.7	19.1	10.2	21.5	3.5	2.630
A–277	Kle	I, 8	47.4	19.0		28.7	4.9	2.668
A–278	Kmgp	F, 1	45.5	17.7		19.8	17.0	2.719
A–280	Kmr	E, 6	41.6	22.5	4.3	28.1	3.5	2.634
A–281	Kmr	E, 6	45.0	21.5	5.6	25.9	2.0	2.616
A–282	Kle	F, 4	48.1	16.9		25.0	10.0	2.687
A–283	Kle	G–H, 5	41.9	24.0		26.3	7.8	2.687
A–284	Kl	H, 4	49.3	15.3		19.4	16.0	2.720
A–285	Kle	G, 4	42.2	20.7		26.4	10.7	2.693
A–286	Ktp	K, 6	41.1	22.7		33.5	2.7	2.691
A–287	Kl	J, 7	50.0	14.7		20.8	14.5	2.729
A–289	Kl	J, 6–7	50.3	14.7		20.6	14.4	2.726
A–290	Kle	J, 8	43.5	18.8		25.4	12.3	2.704
A–291	Kle	J, 8	43.7	21.0		29.4	5.9	2.666
A–293	Klef	J, 8	37.4	30.1		30.9	1.6	2.640
A–295	Klep	K, 8	39.2	28.2		27.0	5.6	2.653
A–304	Ktp	K, 6	49.6	15.8		23.8	10.8	2.703
A–308	Klef	J, 7	43.1	27.8		27.3	1.8	2.639
A–310	Klp	I, 6	45.9	19.0		20.6	14.5	2.701
A312A	KJcl	F, 9	38.4	24.3		25.8	11.5	2.701
A–313	KJcl	E, 8–9	44.9	22.4		19.9	12.8	2.717
A–316	KJcl	E, 9	35.5	27.7		28.6	8.2	2.672
A–403	KJg	F, 3	32.8	34.9		32.0	.3	2.605
A–405	Klef	F, 3	51.8	14.1		21.3	12.8	2.729
A–406	KJg	F, 3	30.3	35.3		32.9	1.5	2.620
A–407	Kl	G, 3	45.4	14.6		22.0	18.0	2.724
A–409	Kl	G, 3	53.3	7.4		20.7	18.6	2.736
A–412	Kqm1	B, 5	35.8	36.8		26.7	.7	2.604
A–413	Kmr	C, 5	45.9	22.7	5.2	22.7	3.5	2.658
A–414	Kmr	C, 4–5	48.5	15.9	7.4	24.2	4.0	2.649
A–420	Kmr	E, 5	44.9	17.7	9.2	24.9	3.3	2.663
A–421	Kmr	G, 6	43.0	21.9	6.8	26.3	2.0	2.661
A–422	Kmr	G, 7	43.5	24.9	3.7	25.0	2.9	2.633
A–425	Kle	G, 5	52.0	15.7		21.4	10.9	2.708
A–426	Kmr	F, 6	44.2	21.1	7.1	22.7	4.9	2.662
A–427	Kmr	F, 6	44.1	17.5	6.1	27.2	5.1	2.650
A–428	Kmr	F, 6	43.2	20.6	5.2	27.3	3.7	2.657
A–429	Klef	H, 5	49.9	11.4		21.3	17.4	2.742
A–430	Kmr	G, 9	41.4	25.8	2.0	29.6	1.2	2.637
A432A	KJcl	F, 9	40.9	22.0		19.8	17.3	2.728
A–433	Kmr	G, 9	41.7	20.3	4.4	30.2	3.4	2.641
A–436	Kmr	H, 9	42.1	21.7	5.3	28.5	2.4	2.640
A–438	Kmr	I, 9	44.4	19.5	6.1	25.9	4.1	2.657
A–439	Kmr	I, 9	39.3	20.3	8.3	24.6	7.5	2.656
A–441	Kmr	G, 9	39.8	26.1	2.4	27.7	4.0	2.639
A–442	KJcl	F, 9	37.4	30.2		20.9	11.5	2.731
A–444	Kqm1	I, 7	37.9	32.1		27.1	2.9	2.628
A–445	Kle	I, 7	55.0	17.3		19.8	7.9	2.729
A–446	Klp	I, 6	29.8	35.0		30.1	5.1	2.634
A–447	Kl	I, 6	49.2	13.8		19.8	17.2	2.754
A–448	Kle	H, 6	44.3	22.2		25.6	7.9	2.701
A–449	Kle	H, 7	42.3	28.2		28.9	.6	2.637
A–450	Kmr	G, 6	49.2	18.0	5.8	23.4	3.6	2.657
A–451	Kmr	D, 6	40.9	25.6	4.3	26.2	3.0	2.627
A–452	Kmr	F, 7	40.0	24.2	4.6	28.5	2.7	2.629
A–453	Kmr	F, 7	44.6	18.8	4.8	27.6	4.2	2.660
A454B	Kle	E, 3	48.8	19.4		21.5	10.3	2.684
A–455	Kle	F, 4	48.1	16.6		23.2	12.1	2.704
A–456	Kle	F, 4	49.9	17.6		19.3	13.2	2.730
A–457	Kle	G, 4	42.2	22.3		29.3	8.7	2.682
A–458	Kle	G, 4	47.0	18.3		21.9	12.8	2.717
A–459	Klef	H, 4	54.4	14.0		21.3	10.3	2.719
A–460	Kmr	G, 6	45.1	17.2	8.2	26.3	3.2	2.660
A–461	Kle	H, 6	44.9	17.5		30.2	7.4	2.674
A–462	Kmr	H, 7	42.9	21.1	9.8	24.7	1.5	2.632
A–463	Kmr	G, 7	44.0	23.0	2.7	27.2	3.1	2.634
A–464	Kmr	F–G, 8	39.8	31.6	2.4	23.7	2.5	2.633
A–465	Kmr	G, 8	41.0	25.6	2.3	27.6	3.5	2.627
A–466	Kle	H, 6	49.2	18.8		20.3	11.7	2.713
A–467	Kl	H, 4	47.1	16.2		22.2	14.5	2.723
A–468	Kl	G–H, 4	52.5	13.8		17.6	16.1	2.750
A–470	KJbd	H, 2	44.4	25.0		24.4	6.2	2.664
A–471	Kl	J, 6	47.2	12.2		20.9	19.7	2.753
A–473	Ktp	K, 6	45.2	17.5		23.5	13.8	2.731
A–474	KJbd	J, 5	51.3	22.8		21.9	4.0	2.690
A–475	Kl	J, 5	53.7	14.2		18.4	13.7	2.771
A–477	KJqd1	K, 6	33.7	34.0		24.2	8.1	2.670
A–479	Kl	I, 5	47.1	18.3		16.5	18.1	2.749
A–480	Kl	H, 5	41.2	19.5		24.2	15.1	2.720
A–481	Kl	J, 6	50.0	16.6		20.2	13.2	2.754
A–482	Kle	J, 9	47.8	19.7		23.1	9.4	2.691
A–484	Kle	K, 9	49.3	16.5		23.4	10.8	2.692
A–485	Kle	K, 9	38.9	23.1		31.0	7.0	2.662
A–486	Kqm1	K, 9	48.9	18.3		26.6	6.2	2.673
A–487	Kle	K, 9	52.4	11.9		19.0	16.7	2.734
A–488	Klp	K, 8	44.5	14.5	4.2	24.7	12.1	2.702
A–489	Kle	K, 8	47.6	17.1		25.4	9.9	2.710
A–490	Kle	J, 8	41.2	25.3		25.3	8.2	2.671
A–491	KJqm	K, 6	39.1	39.6		19.2	2.1	2.621
A–493	KJqd1	K, 6	69.8	2.1		5.9	22.2	2.830
A–495	Ktp	K, 6	71.1	7.1		11.5	10.3	2.699
A–496	Ktp	K, 7	49.1	19.0		24.4	7.5	2.705
A–499	Klp	K, 8	46.9	21.2		19.1	12.8	2.717
A–500	Kl	K, 7	42.3	19.2		25.1	13.4	2.721
A–503	Klp	J, 7	39.4	23.0		26.6	11.0	2.698
A–507	Kle	I, 8	48.4	19.0		23.5	9.1	2.694
A–508	KJbdf	K, 4	40.6	40.2		16.7	2.5	2.644
A–509	KJqd1	K, 4	67.4	.8		10.2	21.6	2.830
A–510	KJbdf	K, 5	54.9	9.3		28.9	6.9	2.647
A–511	KJbd	H, 2	49.7	23.4		19.3	7.6	2.675
A–512	KJbdf	I, 4	31.8	37.2		28.0	3.0	2.612
A–514	KJg	C, 1	35.2	36.3		28.0	.5	2.614
A–515	KJg	B, 1	42.1	33.2		23.1	1.6	2.607
A–518	Kmr	A, 2	46.5	18.0	4.3	27.3	3.9	2.653
A–519	Kmr	A, 3	43.8	18.6	7.6	26.3	3.7	2.656
A–520	Kmr	A, 3	43.9	22.6	5.9	25.0	2.6	2.631
A–521	KJgp	B, 1	26.0	40.4		31.1	2.5	2.622
A–536	KJbdf	J, 2	53.6	34.3		8.7	3.4	2.631
A–538	Kmr	A, 4	42.2	20.7	5.7	29.7	1.7	2.642
A–539	Kqm1	B, 4	53.4	28.8		14.0	3.8	2.652
A–541	KJbdf	J, 3	33.9	38.5		26.0	1.6	2.625
A–542	KJcl	E, 9	39.6	32.3		15.3	12.8	2.693
A–546	KJcl	E, 9	34.0	37.5		21.8	6.7	2.658
A–547	KJqd2	D, 9	71.5	5.4		3.9	19.2	2.835
A–550	KJqd2	E, 9	51.1	17.8		15.5	15.6	2.734
A–552	Kmr	F, 9	37.1	24.8	11.2	22.1	4.8	2.634
A–554	Kmr	F, 8	34.7	22.5	10.3	29.0	3.5	2.628
A–555	Kmr	D, 5	43.3	17.4	7.5	27.8	4.0	2.650
A–556	Kle	E, 5	48.1	18.3		22.6	11.0	2.710
A–558	Klep	G, 5	46.0	23.4		25.0	5.6	2.681
A–559	KJs	C, 2	49.1	19.0		22.0	9.9	2.706
A–561	KJg	C, 3	34.1	44..2		20.4	1.3	2.610
A–562	KJd1	C, 3	61.4	.8		12.7	25.1	2.809
A–563	KJg	C, 3	31.7	40.1		27.4	.8	2.611
A–564	KJg	D, 3	25.1	43.0		31.5	.4	2.619
A–565	Klef	D, 3	43.8	22.1		23.9	10.2	2.695
A–566	KJg	F, 1	22.2	40.3		37.2	.3	2.614
A–567	Kmg	J, 2	43.3	18.2		23.8	14.7	2.720
A–568	KJcl	D, 9	58.9	3.1		9.8	28.2	2.685
A–569	KJqd2	D, 9	38.2	23.9		26.7	11.2	2.858
A–570	KJcl	D, 9	35.8	22.3		26.5	15.4	2.732
A–571	KJrl	D, 9	36.2	31.3		29.2	3.3	2.644

[1]See fig. 1 for location of samples and definition of symbols. See also Lockwood and Lydon (1975) for description.
[2]For Kmr samples, this is the matrix alkali feldspar (megacryst alkali feldspar excluded).
[3]For samples of Kmr only. This value taken from fig. 10.

red dots printed on a transparent base (46 by 38 cm in size) directly over a suitably exposed outcrop and counting those points that fell on megacrysts. Comparison of percentages determined by both methods on the same outcrop (fig. 9) showed that the area-count percentages were consistently too low for sparsely porphyritic rocks and consistently too high for highly porphyritic rocks.

All percentages from the area-count method were then adjusted to agree with the pattern shown by point-count percentages—that is, low percentages were increased, and high percentages were decreased. Thus, for example, a field-determined area count of 5 percent alkali feldspar megacrysts was adjusted to 8 percent before being plotted. These adjusted percentages were used to construct figures 10–12.

The resulting adjusted percentages (386 points—fig.

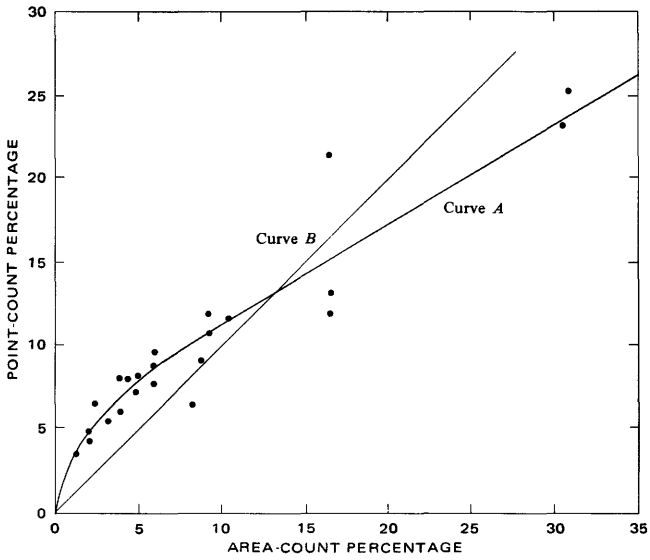

FIGURE 9.—Graph showing relation between point-count and area-count methods of estimating alkali feldspar megacryst abundance in the quartz monzonite of Mono Recesses. Curve *A* is average relation between the two methods. Curve *B* is expected distribution if point-count and area-count methods give equivalent results.

10) were plotted on an overlay of the pluton, and although a distinct pattern of megacryst abundances was observed, there was too much local variation[3] to permit simple contouring of data. To reduce and smooth out the purely local variation, all data were integrated over 1-mi^2 areas on a grid with approximately one-half-mile spacing and then hand contoured. Alkali feldspar megacrysts are concentrated along the southwest margin of the pluton and along most of the northeast margin (fig. 10). The large prong of the pluton that extends to the northeast is composed largely of nonporphyritic alaskite and is considered to represent a late-stage mass of highly differentiated magma that migrated northeastward from the main body of the pluton. Thus, the area of abundant megacrysts in figure 10 that projects across the northeastern prong is considered to mark an earlier margin of the quartz monzonite of Mono Recesses. The increase in abundance of phenocrysts upwards (fig. 11) is similar to the increase near lateral contacts of the pluton, suggesting that the upper contact of the pluton was only a short distance above present erosion levels.

Figure 10 was drafted to facilitate construction of the adjusted modal values of alkali feldspar for the quartz monzonite of Mono Recesses shown in figures 3 and 8, and in table 2. This adjustment was made necessary by the large size (as much as 8 cm long) and irregular local distribution of alkali feldspar megacrysts in the Mono Recesses pluton. Because of the large megacrysts, measured modal compositions of a single sample can vary from intermediate granodiorite to alkali feldspar-rich quartz monzonite, depending solely on where the slab is cut and whether or not large alkali feldspar megacrysts are exposed on the sawn slab. To adjust modes, megacrysts were excluded from the point-count analysis during counting; only fine- to medium-grained alkali feldspar grains in the matrix were counted in the mode, and this is the value reported as "percent alkali feldspar" for samples of the quartz monzonite of Mono Recesses in table 2. For each point at which a modal analysis was available in the quartz monzonite of Mono Recesses, the regional percentage of alkali feldspar phenocrysts was determined from figure 10, and then a new value was obtained for total alkali feldspar, equal to the matrix percentage plus the regional megacryst feldspar percentage. This value is plotted in figure 3 and was used to construct the ternary plots in figure 8.

The alkali feldspar megacrysts are most abundant near the margins of the Mono Recesses pluton (fig. 10). In order to determine whether the abundance of megacrysts reflects the total abundance of alkali feldspar, a plot of the abundance of matrix alkali feldspar versus the abundance of alkali feldspar megacrysts (fig. 12) was constructed. This plot shows a weak inverse correlation between volume percent of matrix and megacryst alkali feldspar in the pluton. Thus the abundance of megacrysts does not simply reflect total abundance of alkali feldspar components in the magma but rather demonstrates that near the pluton margin a physical environment or total magma composition was conducive to growth of the giant crystals.

The modes of specimens of the quartz monzonite of Mono Recesses lie in both the granodiorite and the quartz monzonite fields (fig.8). The modal variation is reflected in the whole-rock chemistry of the rocks, and informal plots of normative quartz, orthoclase, and plagioclase versus lateral position in the pluton for the six analyzed samples of the quartz monzonite of Mono Recesses show that the most calcic rocks are found near the margins of the pluton and the most silicic rocks are found in the center. A corresponding pattern is shown in the variation of specific gravity of samples from the pluton (fig. 7); the densest rocks are found along the margins and the least dense in the center. Thus, the quartz monzonite of Mono Recesses follows the trend of normal zoning (most silicic rocks in the center) found in other granitic plutons. This conclusion is also borne out by the distribution of hornblende, which is restricted to marginal areas of the pluton.

[3]Much of this is apparently variation of megacryst abundance with elevation. In areas of large relief (for example, Mono Creek, where the local topographic relief in places exceeds 2,500 feet) megacryst abundance increases with elevation (fig. 11). This variation related solely to the topography frustrates direct contouring of the data.

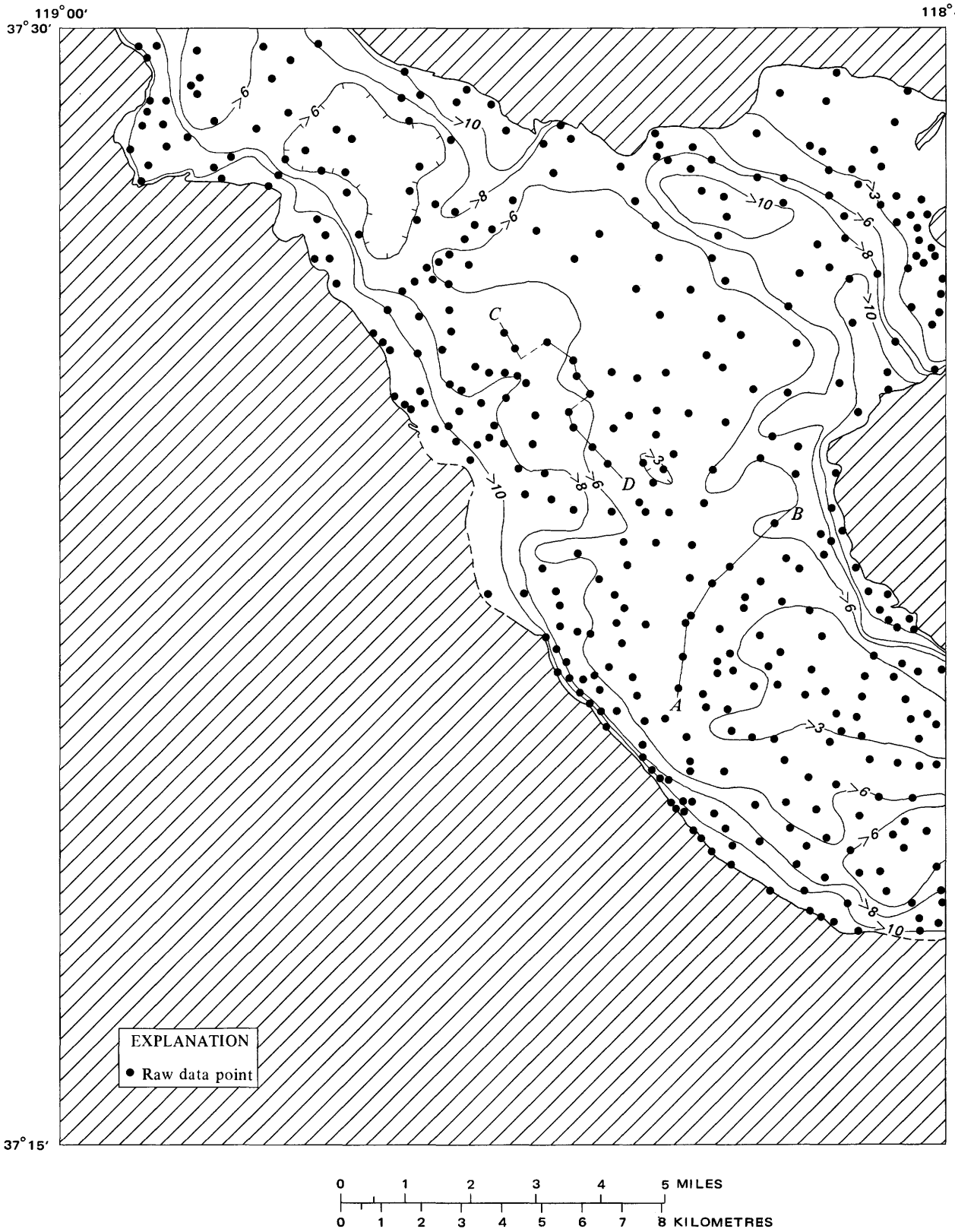

FIGURE 10.—Abundance of alkali feldspar megacrysts in the quartz monzonite of Mono Recesses.

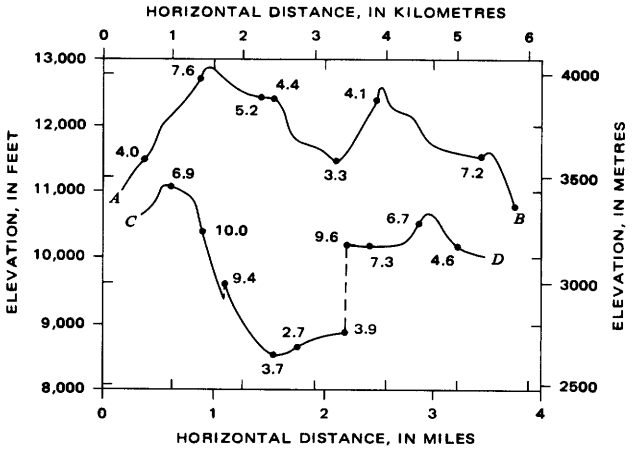

FIGURE 11.—Relation of alkali feldspar megacryst abundances (in percent) to topographic relief in two profiles across the quartz monzonite of Mono Recesses in the Mount Abbot quadrangle.

REFERENCES

Bateman, P. C., Clark, L. D., Huber, N. K., Moore, J. G., and Rinehart, C. D., 1963, The Sierra Nevada batholith—A synthesis of recent work across the central part: U.S. Geol. Survey Prof. Paper 414- D, 46 p.

Bateman, P. C., and Eaton, J. P., 1967, Sierra Nevada batholith: Science, v. 158, no. 3807, p. 1407–1417.

Lockwood, J. P., Bateman, P. C., and Sullivan, J. S., 1972, Mineral resource evaluation of the U.S. Forest Service Sierra Demonstration Project Area, Sierra National Forest, California: U.S. Geol. Survey Prof. Paper 714, 59 p.

Lockwood, J. P., and Lydon, P. A., 1975, Geologic map of the Mount Abbot quadrangle, central Sierra Nevada, California: U.S. Geol. Survey Geol. Quad. Map GQ–1155, scale 1:62,500.

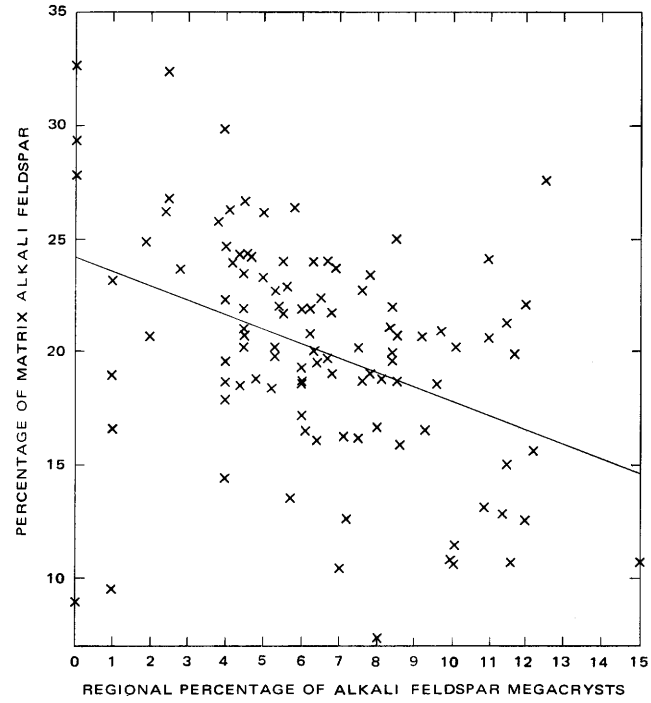

FIGURE 12.—Graph showing variation of alkali feldspar megacryst abundances with matrix alkali feldspar abundances in the quartz monzonite of Mono Recesses. Line is the least-squares best fit solution for the data.

Shapiro, Leonard, and Brannock, W. W., 1962, Rapid analyses of silicate, carbonate, and phosphate rocks: U.S. Geol. Survey Bull. 1144–A, 56 p.

☆ U.S. GOVERNMENT PRINTING OFFICE: 1975-0-690-036/32